A Dynamic Resource Assignment Method for Uncoordinated Wireless Networks

Serkan Uygungelen and Zubin Bharucha
DOCOMO Euro-Labs, Munich, Germany
{uygungelen, bharucha}@docomolab-euro.com

***Abstract*—A dynamic frequency reuse method applicable to uncoordinated and (possibly) dense wireless networks is presented in this paper. The main objective is to protect mobile users located near the cell boundary from detrimental downlink interference originating from neighboring base stations (BSs) without compromising the system spectral efficiency. For this purpose, based on our previous work, a novel dynamic resource assignment method called extended graph based dynamic frequency reuse (eGB-DFR) is developed. The proposed method is designed such that the interference protection does not coincide with an intolerable and unnecessary reduction in the attainable spatial reuse of radio resources. This is achieved by smart defining of two classes of resources depending on their foreseen usage by a BS and assigning them according to the interference environment. The effectiveness of our proposal is corroborated via system-level simulations which reveal that cell-edge capacities are significantly boosted without a sharp decrease in average system throughput.**

I. Introduction

Data traffic has dramatically increased in cellular networks in recent times. The NTT DOCOMO network in Japan has witnessed a near doubling of data traffic within one year, thanks to various video services and high-speed mobile access of smart phones. Countering such a dramatic traffic increase has become one of the most important issues for network operators. NTT DOCOMO launched a commercial long term evolution (LTE) service in 2010 [1]. But it is clear that further countermeasures are needed to keep up with the relentless demand for capacity. It is a well-known fact that a significant fraction of traffic served by a cellular network is located indoors; yet conventional macro-cellular networks, where base stations (BSs) are usually positioned outdoors, may fail to deliver broadband experience to indoor users, due to severe wall penetration losses. As a solution to this problem, low-power BSs such as femto BSs are considered potentially very promising since they can be deployed indoors, and so wall penetration losses are largely mitigated, while the spatial reuse of radio resources is tremendously boosted, due to the small cell sizes [2–4] and low transmit powers. Unlike macro-cellular networks, such small-cell networks are typically randomly deployed without sophisticated planning of the network topology. This causes high co-channel interference between cells, especially in networks where the BSs are densely deployed, such as within public buildings, enterprises or residential apartment complexes.

This work has been performed in the framework of the ICT project ICT-4-248523 BeFEMTO, which is partly funded by the European Union. The authors would like to acknowledge the contributions of their colleagues from the BeFEMTO consortium.

Fractional frequency reuse (FFR), where interfering neighbors transmit data on orthogonal subbands (subbands are contiguous collections of frequency resources) is well known in wireless cellular networks to enhance the throughput of cell-edge users. Access to the remaining subbands is restricted (possibly via power reduction) or even forbidden, so as to avoid detrimental interference with neighboring BSs. Thus, via the use of FFR, user equipments (UEs) located near the boundary of two or more BSs face less interference and enjoy better service quality. However, the disadvantage of using FFR is that it drastically decreases the spatial reuse of resources and hence decreases the system capacity. Additionally, uncoordinated deployment of small cells causes the unpredictable variations in the interference. This indicates the necessity for dynamic frequency reuse approaches that aim at adapting the spatial reuse of resources to the observed interference conditions.

In [5], we have developed a centralized subband assignment scheme for uncoordinated networks named as graph based dynamic frequency reuse (GB-DFR). In GB-DFR, a central controller collects the identity of the interfering neighbors observed by each BS and maps this information onto an interference graph. It then assigns subbands to BSs by applying a modified graph coloring algorithm that takes into account the efficient spatial reuse of subbands. The reader is urged to refer to the paper to glean further details on the procedure. The novelty of GB-DFR stems from the flexibility in the number of subbands that can be assigned depending on the interference conditions observed by each BS. Those BSs facing low interference are assigned more subbands and *vice versa*. However, GB-DFR is suitable only for single user deployments where each BS serves just one UE. As the BS serves more UEs, the utilization of subbands decreases.

In this paper, an extended GB-DFR (eGB-DFR) is proposed that is better suited to serve multi-user scenarios with the objective of increasing the cell-edge capacity whilst maintaining a high subband utilization. In order to enable this, we define two classes of subbands depending on their foreseen usage by a BS: primary subbands (PSs) and secondary subbands (SSs). The PSs are assigned by a central controller similar to GB-DFR [5] and mainly reserved for cell-edge UEs. The PSs belonging to a particular BS cannot be used by their interfering neighboring BSs because such neighbors can cause high interference to UEs of the BS in question. In order to ban/block subbands at the interfering BSs, BSs send a PS indicator to their interfering neighbors. When a BS receives such an indicator, it cannot use the indicated subband and this way cell-edge UEs allocated resources from within the

978-1-4673-1881-5/12/$31.00 ©2012 IEEE

set of PSs experience low interference. Secondly, the SSs, belonging to the set of all unblocked (in other words, non-PS) subbands are assigned autonomously by BSs after PSs are assigned, similar to the method we developed in [6]. SSs can be used by a BS depending on the prevailing interference conditions; but, enjoying no privileges, these subbands cannot be blocked at interfering neighboring BSs. Resources of SSs can therefore be allocated to cell-center UEs facing less interference as long as they do not cause high interference to neighboring BSs. Consequently, the usage of the PSs boosts cell-edge capacity, whereas the SSs increases the spatial reuse of resources especially for multi-user deployments. This is therefore a hybrid method comprising a centralized *and* a decentralized component.

This paper is structured as follows. Section II describes the system model used. A detailed description of eGB-DFR is given in Section III. The simulation setup is explained in Section IV and results are presented in Section V. Finally, Section VI draws conclusions.

II. System Model

As in [5], the downlink of a 3GPP LTE system is considered, where the system bandwidth consists of multiple subbands. Each subband consists of a fixed number of resource blocks (RBs) which are the most basic downlink resource allocation units for data transmission. A BS can allocate RBs of the same subband to multiple UEs, however, any given RB can be allocated to only one UE in a cell.

Owing to the cluttered deployment of BSs, it is impossible for a UE to identify the list of interfering BSs in advance. Instead, a global, pre-defined signal-to-interference-plus-noise ratio (SINR) threshold, γ_{th}, is defined which represents the minimum tolerated SINR for each UE. In LTE, UEs can differentiate between the received signals from various BSs in their vicinity with the help of BS-specific reference signals termed as common reference signals (CRSs). The received signal strength observed by UE_u from BS_n is determined by

$$R_{u,n} = T_{\text{CRS}}\, G_{u,n}, \tag{1}$$

where T_{CRS} is the constant CRS transmit power across all BSs and $G_{u,n}$ is the channel gain comprising the combined effect of path loss and shadowing between BS_n and UE_u.

Based on the received signal strengths from the serving BS, BS_b, and from the set of all interfering BSs, $\mathcal{I}_u$, a UE_u experiences a worst-case SINR of γ_u. If $\gamma_u < \gamma_{\text{th}}$, then from $\mathcal{I}_u$, the largest interfering BS is removed and γ_u is recalculated. This process continues iteratively until

$$\gamma_u = \frac{R_{u,b}}{\sum\limits_{i \in \overline{\mathcal{I}}_u} R_{u,i} + \eta} \geq \gamma_{\text{th}}, \tag{2}$$

where η accounts for thermal noise and $\overline{\mathcal{I}}_u$ is the set of tolerable interfering neighbors defined using set notation

$$\overline{\mathcal{I}}_u = \mathcal{I}_u - \mathcal{I}_{u,\text{rem}}, \tag{3}$$

where $\mathcal{I}_{u,\text{rem}}$ is the set of removed interfering BSs. The set of BSs belonging to $\mathcal{I}_{u,\text{rem}}$ must not use the same subband from which RBs are allocated to UE_u, so that UE_u may achieve an SINR of at least γ_{th}. Based on the feedback received from its served UEs, a BS constructs the union set $\mathcal{I}_{b,\text{rem}}$. This set becomes the neighbor list with regards to the BS in question.

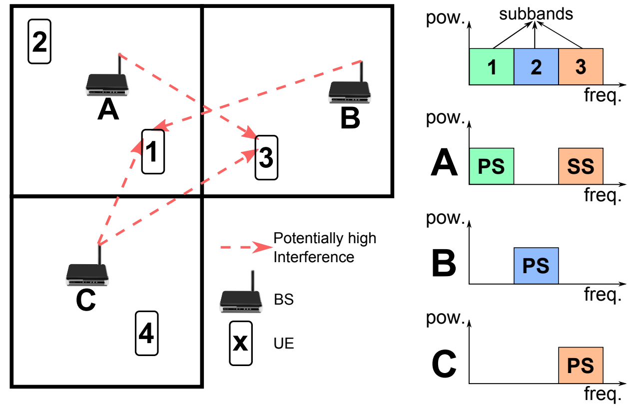

Fig. 1. An example of subband assignment where the system bandwidth consists of 3 subbands.

Furthermore, in LTE, a UE is also capable of calculating the SINR at each subband. Then, it feeds this information back to its serving BS. The signaling of SINR levels is achieved in LTE by using the channel quality indicator (CQI) [7].

III. Extended GB-DFR

The eGB-DFR scheme consists of two parts: central assignment of PSs and autonomous assignment of SSs. Subband assignment is done on an event triggered basis which means subbands are updated only if there is a change in the interference environment. This will be described in detail in the following subsection. Additionally, all BSs are synchronized with a time duration equal to that of a so-called *time slot*. Between the starting instances of two time slots, the subband configuration remains undisturbed, *i.e.*, changes in the subband assignment are only made at the start of the time slots.

A toy example of the allocation of subbands to the various users of various BSs is depicted in Fig. 1. According to this figure, BS_C causes high interference to *some* UEs served by BS_A and BS_B. Since these UEs are allocated RBs from subbands 1 and 2, respectively, these subbands are blocked at BS_C. Likewise, BS_A cannot use subband 2 and BS_B cannot use 1. Therefore, subband 1 is declared the PS for cell A, subband 2 the PS for cell B and subband 3 for cell C. On the other hand, UE_2 served by BS_A does not face high interference from BS_B and BS_C, therefore BS_A may allocate subband 3 RBs to UE_2 without causing high interference to UE_4 served by BS_C.

A BS allocates RBs from PSs and SSs to UEs depending on the UEs' perceived interference conditions. Cell-edge UEs are prioritized for being allocated PS RBs, while the cell-center UEs can be allocated RBs from SS. This results in a fair allocation of resources among UEs in the same cell. For instance, BS_A in Fig. 1, serves UE_1 and UE_2 and can transmit data on subband 1 and subband 3 as PS and SS respectively. As UE_1 faces high interference from BS_C on the SS, only RBs from the PS can be allocated to it. On the other hand, RBs from both PS and SS can be allocated to UE_2. In such a situation, for the sake of fairness, UE_1 gets all resources from the PS and all resources from the SS are allocated to UE_2.

A. Primary Subband Assignment

In order to assign PSs to BSs, the central controller uses an interference graph which is constructed according to the feedback from the BSs. In order to implement this, each BS reports its neighbor list to the central controller when a change (such as the introduction of a new BS to the network) is detected. The central controller then builds an interference graph based on this feedback. If the feedback from BSs causes a change in the interference graph, the central controller updates the PS assignment of all BSs and informs them.

After the PS is assigned, the BS in question can inform the (potential) interfering BSs of its served UEs via a PS indicator. In this way, the serving BS blocks the interfering BSs for using its PS and the desired γ_{th} can be achieved at the given UEs. The serving BS sends PS indicator only for those UEs to which RBs from the PS are allocated, *i.e.*, cell-edge UEs.

1) Construction of the Interference Graph: In the interference graph, each node corresponds to a BS and the edge connecting two nodes represents the interference between two BSs, if this interference exceeds the pre-defined threshold. One important point here is that the edges in the graph are assumed to be undirected, which means that if $\mathrm{BS_A}$ reports $\mathrm{BS_B}$ as its neighbor, then $\mathrm{BS_B}$ automatically becomes the neighbor of $\mathrm{BS_A}$, whether $\mathrm{BS_B}$ reports $\mathrm{BS_A}$ as its neighbor or not. Similar procedures are adopted in [8–10], but neighboring relations are constructed between UEs meaning each node represents a UE in the interference graph. The main advantage of constructing the interference graph based on BSs instead of UEs is that it can remain unchanged for longer periods of time. This way, the update frequency of the PS assignment by the central controller, and hence, the signaling overhead decrease. There are two reasons why the proposed interference graph is stable. Firstly, locations of the BSs do not change frequently. As long as a new BS does not enter the network or the active one does not leave, the nodes in the graph remain same. Secondly, since the BS accumulates feedback from all its served UEs to construct the interference graph, the edges reflect the overall interference conditions experienced by the geographically diverse UEs. Therefore, the movement of one UE does not cause an adverse change to the interference graph, leading to stability. For instance, referring back to Fig. 1, assume $\mathrm{UE_2}$ served by $\mathrm{BS_A}$ changes its location such that it starts to face high interference from $\mathrm{BS_B}$. This, however, does not affect the interference graph since $\mathrm{UE_1}$ already faces high interference from $\mathrm{BS_B}$ which in turn does not change the relation between $\mathrm{BS_A}$ and $\mathrm{BS_B}$ in the interference graph.

As a final remark, increasing γ_{th} results in a graph with higher connectivity, since this increases the number of the neighbors, and hence, the number of edges in the graph. This way, higher SINRs are achieved, but this is traded off with a reduced spatial reuse of subbands.

2) Graph Coloring Algorithm: Conventional graph coloring algorithms, such as the one given in [11], color the nodes of a graph with the minimum number of colors such that no two connected nodes (in this context, neighbor nodes) have the same color. By assuming that each color represents a different subband, graph coloring facilitates subband assignment, where two BSs connected via an edge in the interference graph cannot use the same subband.

The drawback of conventional graph coloring is the inefficient usage of the subbands since each BS is assigned only one subband. In order to increase the spatial reuse of subbands, a BS in a less interfering environment should be able to use more subbands without causing high interference to its neighbors. Shortcomings of conventional graph coloring are addressed in [5] with the proposed GB-DFR scheme, where the subbands are assigned to BSs in three steps and a cost function is introduced to maximize the spatial reuse of subbands. Additionally, in order to increase the fairness for situations where the number of subbands is high, a parameter $s_{\min}$ is introduced. It indicates the minimum number of subbands that should be assigned to each BS. The GB-DFR can be summarized as (for more details, the reader may refer to [5]):

- **Step 1: Assigning $s_{\min}$ subbands to BSs**
  - Apply the graph coloring algorithm $s_{\min}$ times to the interference graph.
  - For each visited BS assign the optimal subband in terms of utilization of subbands.
- **Step 2: Assigning the remaining subbands to BSs**
  - For each subband, find out the BSs to which the given subband can be assigned.
  - Choose the optimal BS in terms of utilization of subbands.
- **Step 3: Find out BSs without any assigned subband**
  - If there is any BS which is not assigned any subband because of intense interference, assign a subband causing minimum interference to its neighbors.

The first step of the GB-DFR is quite similar to the conventional graph coloring algorithm, however it assigns $s_{\min}$ subbands to BSs instead of one. This is achieved by applying the graph coloring algorithm to the interference graph $s_{\min}$ times. The rest of the subbands are assigned to BSs during the second step by choosing the most optimal BS in terms of the usage utilization of subbands. Finally, the third step searches for the BSs which are not assigned any subband because of intense interference environment and assigns a subband causing minimum interference to their neighbors. For more details, the reader may refer to [5].

The GB-DFR method efficiently solves the issue of assignment of subbands for the dynamic environment arising from the cluttered deployment of BSs and allows for UE movement. Also, since the number of nodes is relatively small, the proposed algorithm has low time complexity for the given interference graph and hence the central controller can update the subband assignment with a bearable delay. Note that the complexity does not increase as the number of served UEs increases. Additionally, the rate of change of the interference graph is low which reduces the need for the central controller to update the subband assignment frequently. Consequently, applying the GB-DFR by a central controller is a convenient approach for assigning PSs to BSs. It is guaranteed that the interfering BSs use different PSs as long as the interference graph remains unchanged. However, assigning all subbands as a PS and restricting all potential interfering neighbors decreases the spatial reuse of subbands for multi-user deployments. For example, assume some BS_b is assigned multiple subbands, say subbands 1 and 2, after applying the

GB-DFR. This forbids all its neighbors in the interference graph from using these subbands which protects the cell-edge UEs of BS_b. However, for cell-center UEs that do not need protection, BS_b does not need to restrict its neighbors. So that if BS_b uses subband 1 for cell-edge UEs and subband 2 for the cell-center UEs, then the neighbors of BS_b are not blocked from using subband 2. In this way, more subbands can be utilized. This gives an indication as to why we need to classify subbands as PSs and SSs. For this purpose in eGB-DFR, we apply only the first and third steps of the GB-DFR for assigning PSs by setting $s_{\min}$ as the number of PS per BS. The rest of the subbands are assigned as a SS autonomously by BSs, the procedure of which is explained in the sequel.

B. Secondary Subband Assignment

Similar to PSs, the same γ_{th} is set for SSs which means a BS can assign a subband as a SS if any of its served UEs experiences an SINR higher than γ_{th} on the given subband. For the SS assignment, a BS gets feedback from the central controller (if its PS is updated), its neighboring BSs and its served UEs. When the BS receives an updated PS information from the central controller, it gives up its assigned SSs. This is because, the central controller updates the PS assignment without knowing the SS assignment. So, the BS should re-assign SSs according to the updated PS assignment. However, as explained in the previous subsection, the PS assignment remains the same for longer periods of time, which means that the BS does not need to reset all its assigned subbands frequently. For the time slots when the BS does not receive a PS update from the central controller, it computes the SS assignment for the next time slot, based on the feedback received by it from its served UEs and neighboring BSs in the previous time slot. This procedure is clarified via Fig. 2 which shows an overview of the autonomous assignment of SSs applied by BS_A at the start of a time $t+1$ (assuming that feedback has been received in time slot t).

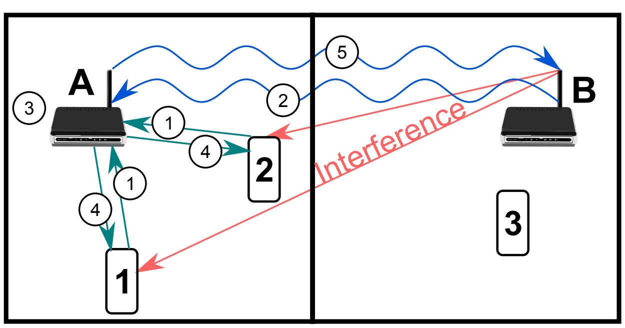

Fig. 2. Overview of the autonomous assignment of SSs applied by BS_A. The arrows are numbered to indicate the order of the procedures.

According to the figure, BS_A acts as a sink for collecting SINR levels on every subband from its associated UEs, ① and PS indicators from neighboring BSs, which is used for signaling the PS information to the interfering neighbors ②. Depending on the reported feedback from the time slot t, BS_A updates its subband assignment for the time slot $t+1$, ③ and from this allotment of subbands, downlink RBs are allocated to the served UEs, ④ and a PS indicator is sent to the corresponding interfering BSs ⑤. The same procedure is followed by all BSs in the network. All the subband selection processes are explained in the following subsections.

1) Set of Available Subbands for Transmission: A BS needs to use a metric to choose the most efficient subband in terms of a desired performance criterion. For this purpose, a metric termed as *subband availability* is introduced. The availability of a subband indicates how many UEs experience an SINR higher than γ_{th} on that subband in a given cell. However, if a BS receives a PS indicator from its neighbor(s), the given BS cannot use that subband. Therefore, in this case, the availability of the subband becomes 0 independent of the SINR levels reported by UEs. The calculation of the availability of s in BS_b is as

$$A_{s,b} = \begin{cases} \sum_{u\in\mathcal{U}_b} \mathbb{1}(\gamma_u^s \geq \gamma_{\text{th}}) & \text{if } s \text{ is not blocked} \\ 0 & \text{if } s \text{ is blocked} \end{cases} \tag{4}$$

where $\mathbb{1}(.)$ is a conditional binary function whose output is 1 if its argument holds true and 0 otherwise. Here, γ_u^s is the SINR at subband s measured by UE_u and $\mathcal{U}_b$ is the set of all UEs served by BS_b.

2) Assignment of Idle Subbands: Since the SS assignment is determined by a BS based on UE feedback, which inherently induces latency, it is possible that multiple BSs access the same subband giving rise to destructive interference. The occurrence of such failed subband assignments decreases as BSs learn the nature of their environment and the network reaches a stable point where BSs no longer need to update their subband assignments. Moreover, frequent changes in subband assignments creates a cascading effect whereby neighboring BSs are to update their subband selection, which increases the time required to reach a stable resource assignment. Therefore, we introduce a p-persistent slot allocation in SS assignment. In p-persistent slot allocation policy [12], when a channel is sensed idle by a transmitter, meaning no other transmitters send any packet, the transmitter sends the packet with a probability of p. In a similar manner, in eGB-DFR, an idle subband may be assigned with a certain probability depending on the subband's availability. For a given subband s, if a UE reports an SINR higher than γ_{th}, then BS_b assigns s with a probability of p. If multiple UEs experience an SINR higher than γ_{th}, which means availability of s, $A_{s,b}$, is greater than 1, then BS_b applies the p-persistent protocol $A_{s,b}$ times. The probability of the assigning s by BS_b for the next time slot $t+1$ can be formulated as:

$$P_{s,b}(t+1) = 1 - (1-p)^{A_{s,b}} \tag{5}$$

A BS updates its subband assignment only if the probability condition in (5) holds, so that simultaneous assignment of the same subband by interfering BSs becomes less likely. The subband selection therefore converges quicker to a stable state. In (5), it is obvious that the probability of assigning a subband increases as subband's availability increases. This favors the selection of a subband that can be allocated to more users with high SINRs.

3) SS Selection Algorithm: The idea of using SSs is to allocate more resources to cell-center UEs as has already been mentioned. Therefore, a BS searches for subbands on which cell-center UEs experience high SINR. This gives a BS the freedom to use more subbands for UEs facing less interference. However, the assigned subband should not interfere with the PSs of neighboring BSs. The SS selection algorithm applied by BS_b for time slot $t{+}1$ is given in Algorithm 1, where $\mathrm{SS(t)}$ is the set of SSs used in the previous time slot t, PS is the PS assigned by the central controller and $\mathcal{S}$ is the set of all subbands.

Calculate the availability of all subbands
$\mathcal{S} \setminus \{\mathrm{SS(t)} \cup \mathrm{PS}\} \leftarrow \mathcal{S}^{'}$
$\mathrm{SS}(t) \setminus \{s \in \mathrm{SS}(t) | A_{s,b} = 0\} \leftarrow \mathrm{SS}(t+1)$
for $i = 1 \rightarrow |\mathcal{S}^{'}|$ **do**
    $s = \mathcal{S}^{'}(i)$
    if $A_{s,b} > 0$ **then**
        with a prob. of $P_{s,b}(t+1)$: add s to $\mathrm{SS(t+1)}$
    end if
end for

Algorithm 1: SS Selection

The SS selection algorithm first calculates the availability of all subbands using (4). Additionally, before selecting any SS, the BS discards the subbands having zero availability from the SS set, $\mathrm{SS(t+1)}$, because either these subbands are banned by the neighboring BSs via a PS indicator or all UEs in the cell experience SINRs lower than γ_{th} over these subbands. Therefore, such subbands cannot be used for the next time slot $t+1$. Then, in the set of subbands which are not assigned as a PS or SS, $\mathcal{S}^{'}$, the subbands having an availability higher than 0 are assigned as a SS with a probability that is calculated using (5).

IV. Simulation Setup

The simulated scenario consists of a single one-story building, modeled by a $5{\times}5$ grid, according to 3GPP specifications [13]. The $5{\times}5$ grid represents a square building consisting of 25 regularly arranged square-shaped apartments. Every apartment hosts a femto BS with a certain *activation probability*. If an apartment contains an active femto BS, it serves a certain number of UEs which are randomly distributed within the confines of the apartment. Full-buffer transmission is assumed such that every BSs assign all available resources from all available subbands to their served UEs. For the sake of simplicity, interference from the macrocell network is neglected, which may be accomplished by allocating different frequency bands to macro and femto BSs. The system parameters summarized in Table I are based on LTE specifications [13].

For throughput calculations, the attenuated and truncated Shannon bound is applied, which approximates the spectral efficiency of appropriately selected modulation and coding schemes subject to the achieved SINR. Detailed information on throughput calculations can be found in [5, 6]. As a final remark, each snapshot of the simulator lasts for 10 time slots. During the snapshot, positions and shadowing values of BSs and UEs are assumed to remain unchanged. This is reasonable since indoors, the mobility of users is not as high as would be the case for outdoors. The statistics, such as SINR and capacity, are calculated at the end of the 10^{th} time slot, *i.e.*, when a stable resource allocation is achieved.

TABLE I
System Parameters

Parameter	**Value**
System Bandwidth	20 MHz
Number of Subbands	4
Min. Sep. between UE and BS	20 cm
BS Antenna Gain	0 dBi
Antenna Pattern (Horizontal)	$A(\theta) = 0\,\mathrm{dB}$ (omnidirectional)
Interior Path Loss	$L = 127 + 30\log_{10} d$ [km], where d is the distance between UE and BS
Shadowing Std. Dev.	10 dB
Max Tx Power	10 dBm
Thermal Noise Density	$\eta = -174\,\mathrm{dBm/Hz}$
UE Noise Figure	9 dB
Apartment Dimensions	$10\,\mathrm{m} \times 10\,\mathrm{m}$
Number of UEs per Femto BS	4
Femto BS Activation Prob.	0.2
SINR Threshold	$\gamma_{\mathrm{th}} = 5\,\mathrm{dB}$
Prob. p in (5)	0.25

V. Results

The performance of eGB-DFR is compared to FFR and GB-DFR. We use two FFR schemes: FFR 1/4 and FFR 2/4 where each BS is centrally assigned one and two subbands out of four available subbands respectively. For eGB-DFR, the number of PS per BS is set as 1.

Fig. 3 shows the cumulative distribution function (CDF) of the achieved SINR. With eGB-DFR and GB-DFR, nearly all UEs achieve an SINR exceeding $\gamma_{\mathrm{th}}{=}5\,\mathrm{dB}$. It is seen that the best SINR performance is achieved by the system where each femto BS only uses one out of four available subbands.

Fig. 4 compares the CDFs of user capacity of the four methods. Due to the truncated Shannon bound, spectral efficiencies saturate at the SINR of $19.5\,\mathrm{dB}$ which is the maximum SINR value that can be used by the available modulation and coding schemes. Additionally, the value at which the saturation occurs depends on the number of resources available for allocation. As a result, despite the encouraging SINR performance exhibited by the system employing FFR 1/4, the capacity saturates at a mere $5.5\,\mathrm{Mbps}$, implying that a high proportion of resources remain unused. While the saturation capacity of FFR 1/4 is doubled over FFR 2/4, occasionally idle resources remain unused. Moreover, the cell-edge user throughput (given by the low percentiles of the user capacity CDF) substantially degrades. eGB-DFR, like FFR 1/4 shows very good cell-edge performance (at the low capacity regime), but also shows very promising cell-center performance at the high capacity regime. These improvements come at a loss of capacity approximately between 30^{th} and 60^{th} percentiles compared to FFR 2/4. However, this loss is compensated by the cell-edge improvements and increase in capacity beyond the 80^{th} percentile. Fig. 4 also shows the superiority of eGB-DFR over GB-DFR at high capacity regions. Since SSs are not blocked, more subbands are utilized with eGB-DFR, hence, cell-center UEs can be allocated more resources.

The improvements in overall performance are summarized in Table II, which compares the cell-edge capacity (defined as the 5% of the CDF of user capacity) and the average cell

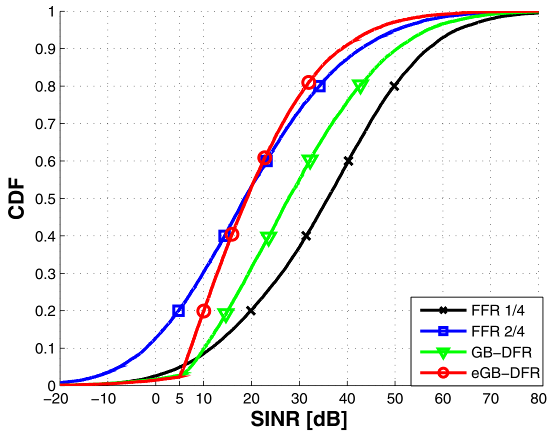

Fig. 3. CDF of SINR

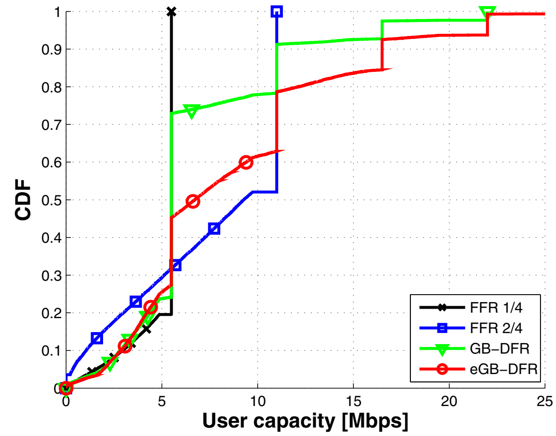

Fig. 4. CDF of User Capacity

capacity. The results demonstrate that eGB-DFR significantly outperforms FFR and GB-DFR in terms of cell-edge and average cell capacity. Therefore, eGB-DFR boosts cell-edge capacity without compromising the system capacity.

TABLE II
PERFORMANCES OF THE COMPARED METHODS

Method	Cell-edge Cap.	Average Cell Cap.
FFR 1/4	1.57 Mbps	19.82 Mbps
FFR 2/4	0.35 Mbps	30.23 Mbps
GB-DFR	1.90 Mbps	27.15 Mbps
eGB-DFR	1.96 Mbps	35.17 Mbps

VI. CONCLUSION

The main contribution of this work is to assign resources in unplanned wireless networks that are characterized by varying interference conditions. The proposed eGB-DFR method takes the advantages of both central and autonomous resource assignment approaches. By assigning the PSs centrally, the system reaches a stable resource assignment in a short time and the cell-edge UEs are well-protected. Additionally, by assigning SSs autonomously, a BS gets more flexibility in choosing subbands available for transmission which increases the utilization of subbands. Simulation results demonstrate that eGB-DFR attains a significant improvement for both cell-edge as well as system capacities, compared to conventional centralized frequency reuse methods and GB-DFR. As the method relies on the measurements of UEs, it is able to dynamically adapt to the interference conditions faced in random deployments, thus balancing high spatial reuse of subbands with interference protection for cell-edge users. Furthermore, the method has less signaling overhead as existing LTE signaling procedures are used. Finally, it is worth mentioning that the use of eGB-DFR is not limited to the frequency-domain as shown in this paper, but can be used with any other domain such as the time- or code-domains.

ACKNOWLEDGMENT

The authors would like to thank Gunther Auer and Hidekazu Taoka for their valuable comments and feedback.

REFERENCES

[1] NTT DOCOMO, “DOCOMO to Launch “Xi”, Japan’s First LTE Service,” http://www.nttdocomo.com/pr/2010/001494.html, November 2010.

[2] H. Claussen, “Performance of Macro- and Co-Channel Femtocells in a Hierarchical Cell Structure,” in *Proc. of the 18th IEEE International Symposium on Personal, Indoor and Mobile Radio Communications (PIMRC)*, Athens, Greece, Sep. 3–7 2007, pp. 1–5.

[3] Z. Bharucha, H. Haas, A. Saul, and G. Auer, “Throughput Enhancement through Femto-Cell Deployment,” *European Transactions on Telecommunications*, vol. 21, no. 4, pp. 469–477, Mar. 31 2010, (invited).

[4] V. Chandrasekhar, J. Andrews, and A. Gatherer, “Femtocell Networks: A Survey,” *IEEE Communications Magazine*, vol. 46, no. 9, pp. 59–67, 2008.

[5] S. Uygungelen, G. Auer, and Z. Bharucha, “Graph-Based Dynamic Frequency Reuse in Femtocell Networks,” in *Proc. of the 73rd IEEE Vehicular Technology Conference (VTC)*, Budapest, Hungary, May 15–18 2011.

[6] S. Uygungelen, Z. Bharucha, and G. Auer, “Decentralized Interference Coordination via Autonomous Component Carrier Assignment,” in *Proc. of the 54th IEEE Global Telecommunications Conference (GLOBECOM)*, Houston, USA, Dec. 5–9 2011.

[7] 3GPP, “Evolved Universal Terrestrial Radio Access (E-UTRA); Physical Layer Procedures (Release 9),” 3GPP TS 36.213 V 9.1.0 (2010-03), Mar. 2010.

[8] R. Chang, Z. Tao, J. Zhang, and C.-C. Kuo, “A Graph Approach to Dynamic Fractional Frequency Reuse (FFR) in Multi-Cell OFDMA Networks,” in *Proc. of the IEEE International Conference on Communications (ICC)*, Jun. 14–18 2009, pp. 1–6.

[9] M. C. Necker, “Integrated scheduling and interference coordination in cellular OFDMA networks,” in *Proc. of the Fourth International Conference on Broadband Communications, Networks and Systems (BROADNETS)*, Sep. 10–14 2007, pp. 559–566.

[10] ——, “A Graph-Based Scheme for Distributed Interference Coordination in Cellular OFDMA Networks,” in *Proc. of the IEEE Vehicular Technology Conference (VTC)*, May 11–14 2008, pp. 713–718.

[11] D. Brélaz, “New Methods to Color the Vertices of A Graph,” *Communications of the ACM*, vol. 22, no. 4, pp. 251–256, Apr. 1979.

[12] L. Kleinrock and F. Tobagi, “Packet Switching in Radio Channels: Part I–Carrier Sense Multiple-Access Modes and Their Throughput-Delay Characteristics,” *IEEE Transactions on Communications*, vol. 23, no. 12, pp. 1400–1416, Dec. 1975.

[13] 3GPP, “Simulation Assumptions and Parameters for FDD HeNB RF Requirements,” 3GPP TSG RAN WG4 R4-092042, May 2009 from www.3gpp.org/ftp/Specs/.